

OTR BEAM PROFILE MONITOR AT ALS/ALS-U*

C. Sun[†], J. De Chant and C. Steier, Lawrence Berkeley National Laboratory, Berkeley, USA

Abstract

Optical Transition Radiation (OTR) is a well-established diagnostic technique for high-resolution beam profile measurements in accelerator facilities. This work reports on the development and testing of OTR-based beam profile monitors for the transfer lines at the Advanced Light Source (ALS) and its upgrade (ALS-U). The objective is to minimize radiation generated by diagnostic screens while enabling online, high-resolution beam characterization. We present key design considerations for OTR screens, including material selection, optical properties, and mechanical integration, along with experimental results from tests at ALS. Performance is evaluated in terms of spatial resolution, signal-to-noise ratio, and linearity with beam current. The results demonstrate that OTR profile monitor can be a promising and easy-to-implement alternative to existing scintillator-based ones and their implementation could provide improved, real-time beam quality control at the ALS and ALS-U.

INTRODUCTION

Beam Profile Monitors are essential diagnostic tools for accelerator commissioning, tuning, and routine operation. In single-pass transfer lines it most commonly employ scintillator screens, which interact with the charged particle beam, converting its energy into visible light that can be imaged with a camera. At the Advanced Light Source (ALS), Chromox-6 scintillator-based beam profile monitors have been in operation since commissioning nearly 30 years ago [1]. This system has provided invaluable information for injector and transfer line tuning, and its applicability has been evaluated for the ALS Upgrade (ALS-U).

Despite their utility, the scintillator-based beam profile monitors are destructive to the beam, generate significant background radiation while in operation, and offer limited spatial resolution. Optical Transition Radiation (OTR) provides a promising alternative and a simple replacement for existing Beam Profile Monitors at the ALS [2]. With appropriate design, OTR-based profile monitors offer higher spatial resolution, reduced background radiation, and the potential for quasi-online measurements.

We are implementing OTR screens for ALS and ALS-U. Key design considerations include screen material, optical properties, and integration with existing designs. Experimental results from ALS tests are presented, evaluating spatial resolution, signal-to-noise ratio, and linearity with bunch charge. These developments are expected to significantly improve beam quality control at the ALS and ALS-U.

OPTICAL TRANSITION RADIATION

When a relativistic charged particle beam crosses the interface between two media with different dielectric constants—typically from vacuum to a metallic foil—it emits radiation. A portion of this radiation falls in the visible range, allowing capture by standard optical systems. The resulting image provides a measurement of the beam's transverse spatial distribution. The intensity distribution at the image plane can be expressed as [3]:

$$I(x, y) \propto \left[\int_0^{\theta_{\max}} \frac{\theta^2}{\theta^2 + \gamma^{-2}} J_1 \left(\frac{k\theta \sqrt{x^2 + y^2}}{M} \right) d\theta \right]^2, \quad (1)$$

where $k = 2\pi/\lambda$ is the wave number with λ the radiation wavelength, x and y are the transverse coordinates at the imaging plane, M is the magnification of the imaging system, θ is the OTR emission angle, γ is the Lorentz factor of the particle beam, θ_{\max} is the collection angle defined by the lens aperture, and J_1 is the first-order Bessel function.

Point Spread Function

Equation (1) incorporates angular distribution, optical aperture, and diffraction, and is widely used to model the point-spread function (PSF) of an OTR-based beam profile monitor. The $1/\gamma$ dependence reflects the relativistic narrowing of the OTR emission cone, while the Bessel function captures the Fourier transform relationship between angular distribution and image-plane intensity.

For a 1.9 GeV electron beam, the calculated intensity distribution at the imaging plane exhibits an RMS width of approximately $2\mu\text{m}$ as shown in Fig. 1. For beams with sizes of a few tens to hundreds of micrometers, this result indicates that the intrinsic resolution of the OTR screen is not constrained by the emission itself, but instead by the optical performance of the imaging system, which plays a dominant role.

Sensitivity

The main limitation of OTR is its relatively weak emission intensity compared to scintillators, requiring higher-sensitivity cameras and carefully designed imaging system. In addition, because the foil must intercept the beam, the measurement is inherently invasive and can introduce scattering. However, the perturbation to the beam can be minimized with the use of very thin foils, allowing OTR monitors to provide online measurements during beam operation.

The weak emission challenge can be mitigated by modern camera technology. Advanced CCD and CMOS cameras provide sufficient sensitivity for OTR detection. To evaluate the sensitivity requirements, one can estimate the number of photons collected by the imaging system. Since the photons are distributed across many pixels on the image plane, the

* Work supported by the Director Office of Science of the U.S. Department of Energy under Contract No. DE-AC02-05CH11231

[†] ccsun@lbl.gov

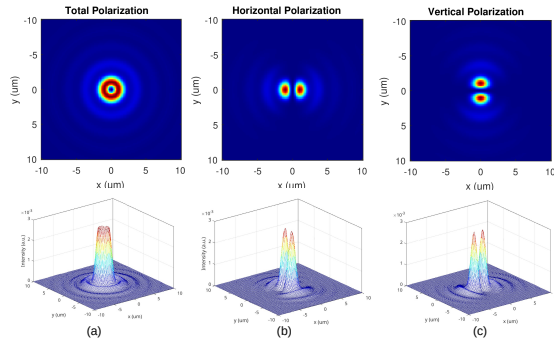


Figure 1: Calculated point spread function at the imaging plane of the proposed OTR-based profile monitor: (a) Total polarization, (b) Horizontal polarization, (c) Vertical polarization.

key parameter is the maximum number of photon-electron N_e generated on a single pixel of the camera, which can be estimated as a function of bunch charge Q in nC [4]:

$$N_e \approx 4.6 \times 10^6 Q \frac{\Delta x \Delta y}{\sigma_x \sigma_y} \ln \left| \frac{\lambda_2}{\lambda_1} \right| \ln(\gamma \theta_0) Q_E, \quad (2)$$

where $\Delta x, \Delta y$ are pixel dimensions, σ_x, σ_y the beam size, $\lambda_1 - \lambda_2$ the working wavelength range, Q the bunch charge in nC, Q_E the camera quantum efficiency, and θ_0 the collection aperture radius.

For ALS/ALS-U parameters, $E = 2.0$ GeV, $\theta_0 = 127$ mrad, wavelength range 470–645 nm, $Q_E = 0.15$, pixel size $\Delta x = \Delta y = 6.4 \mu\text{m}$, beam size $\sigma_x = \sigma_y = 350 \mu\text{m}$, the estimated photon-electron counts per pixel for different bunch charges at different sigma are shown in Table 1. With a scientific digital camera such as the Manta G-235 (sensitivity threshold $7.2 e^-$), reliable beam profiles can be obtained for bunch charges as low as 0.2 nC.

Table 1: Photon-electron Counts at varying Bunch Charges

Bunch charge (nC)	0.2	0.5	1	30
Peak (e-)	114	227	453	13600
2-sig (e-)	16	31	61	1840
3-sig (e-)	1	2	5	151

Screen Material

OTR screens can be made of different materials and with varying thickness to balance signal intensity, durability, and minimal beam disturbance. For the ALS/ALS-U, thin aluminum foils are used to minimize beam perturbation. The foil is stretch-mounted on a frame with vacuum-compatible epoxy [5], and the beam-facing surface is polished to a mirror finish to minimize scattering. Since OTR is emitted as a directed and narrow cone, precise optical alignment is required to ensure efficient light collection and accurate beam profile measurements.

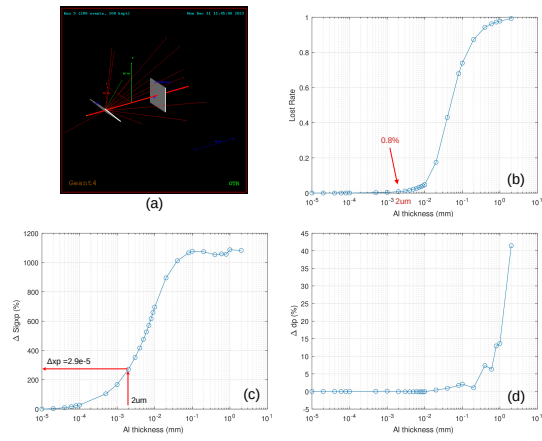


Figure 2: Geant4 Simulation: (a) Setup, (b) Loss rate, (c) Divergence relative to the nominal value of 1×10^{-5} , (d) Energy spread relative to the nominal value of 1×10^{-3} .

GEANT4 SIMULATION

Geant4 [6] simulations were performed to evaluate the impact of the OTR screen on the beam and optimize its thickness. The simulation, illustrated in Fig. 2, models a relativistic electron beam incident on a thin aluminum foil. The primary goals were to quantify beam loss, emittance growth, and energy spread introduced by the foil.

The results, shown in Fig. 2, indicate that a very thin foil (a few micrometers) is optimal. For an aluminum foil $2 \mu\text{m}$, the beam loss rate is minimal ($< 1\%$), the induced divergence is negligible and the energy spread degradation is acceptably low. This confirms that a thin aluminum foil can serve as a minimally invasive diagnostic tool for high-energy electron beams at the ALS/ALS-U.

MECHANICAL DESIGN AND INTEGRATION

The mechanical design of the OTR monitor was guided by the need for robustness, compactness, and compatibility with the existing ALS and ALS-U profile monitors. The key component is a $2 \mu\text{m}$ thick aluminum foil mounted on a dedicated screen holder (Fig. 3), designed to be interchangeable with the chromox-6 scintillator. The holder positions the foil at a 45° angle relative to the beam axis, directing the OTR light perpendicularly out of the beamline toward an imaging viewport.

The screen holder is mounted on a pneumatic rotary actuator to remotely insert the foil into the beam path and remove it when not in use. All of the optics are commercially available components. This design allows the OTR monitor to directly replace existing scintillator-based screens with minimal modification to the vacuum chamber, providing a straightforward upgrade path for the current ALS/ALS-U transfer lines.

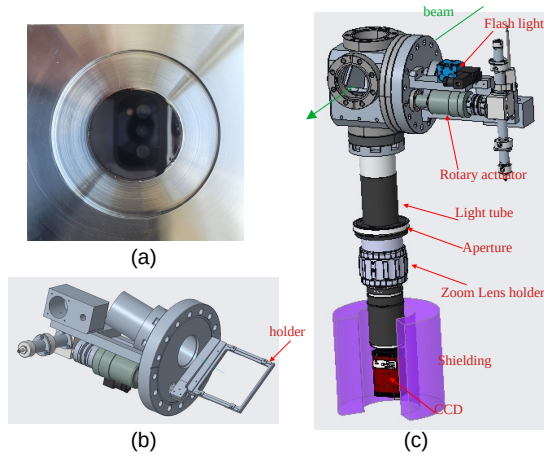


Figure 3: Mechanical design of the OTR screen: (a) $2\ \mu\text{m}$ aluminum foil mounted in an aluminum frame, (b) screen holder and pneumatic rotary actuator assembly, (c) Full assembly and imaging system. The camera is shielded from radiation using xx mm of yy.

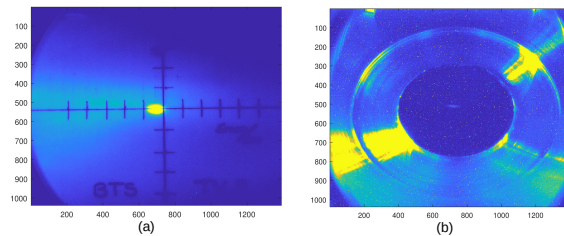


Figure 4: Beam profiles measured with (a) 2 mm Chromox-6 scintillator and (b) $2\ \mu\text{m}$ aluminum OTR screen.

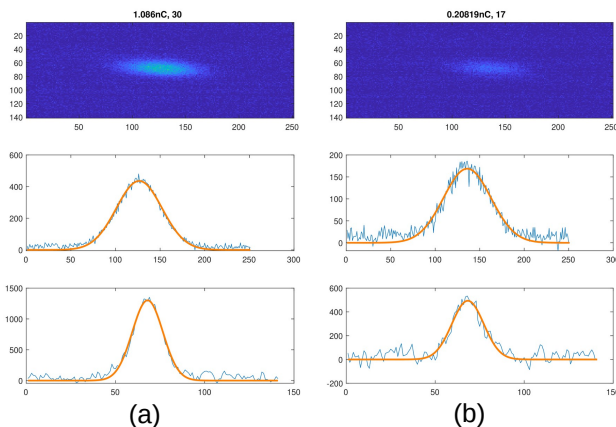


Figure 5: Beam profile with beam charge of (a) 1 nC (b) 0.2 nC.

MEASUREMENT

The OTR monitor was tested on the Booster-to-Storage Ring (BTS) transfer line at ALS, with its performance directly compared against a Chromox-6 scintillator screen under similar beam conditions. A comparison of the beam profiles measured by the two screens is shown in Fig. 4. While the beam profile measured with the OTR screen ex-

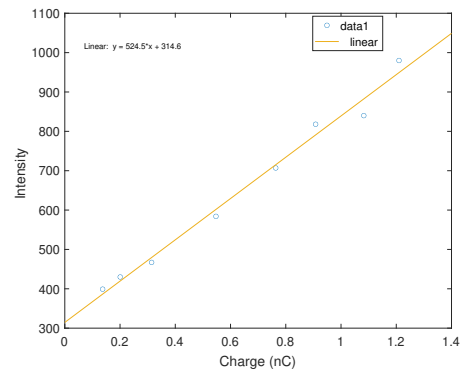


Figure 6: Linearity of the OTR signal with the bunch charge. The integrated profile intensity shows a linear dependence on the bunch charge.

hibits weaker intensity, it remains clearly observable and provides significantly improved spatial resolution.

Figure 5 presents beam profiles obtained at 1 nC and 0.2 nC, demonstrating the monitor's sensitivity even at lower charges. The linearity of the response was evaluated by plotting the integrated profile intensity as a function of bunch charge (Fig. 6), with the results showing good linear agreement. Unlike scintillator-based screens, OTR screens do not suffer from saturation effects or long decay times, making them suitable for measuring high-intensity and high-repetition-rate beams.

CONCLUSION

We have successfully developed, simulated, and tested an OTR beam profile monitor for use in the ALS and ALS-U transfer lines. The design, featuring a $2\ \mu\text{m}$ aluminum foil, was optimized through Geant4 simulations to minimize the impact on beam. The mechanical integration allows it to replace existing scintillator screens with minimal effort. Experimental results confirm the advantages of OTR over traditional scintillators including a higher spatial resolution, a higher dynamic range, and good linearity across a wide range of beam charges from 0.2 nC to 30 nC.

Future work will study OTR foils of varying thickness through simulations and measurements to confirm reduced radiation backgrounds and enable non-destructive online monitoring. Screen material and surface finish will be optimized for higher sensitivity, while mechanical upgrades, such as replacing the pneumatic actuator with a linear stage will improve precision and reliability. Continued deployment in ALS transfer lines will refine these approaches, with the ultimate goal of fully integrating OTR into ALS-U for low-radiation, high-resolution, high-sensitivity, real-time beam profile monitoring.

ACKNOWLEDGMENTS

The authors would like to thank the ALS and ALS-U beam physics and engineering teams for their invaluable support and collaboration.

REFERENCES

- [1] C. H. Kim and J. Hinkson, “Advanced light source instrumentation overview”, *AIP Conf. Proc.*, Vol. 281, pp. 101-119, 1992. doi:10.1063/1.44354.
- [2] B. Gitter, “Optical Transition Radiation”, UCLA, Los Angeles, CA, USA, Rep. CAATECH-NOTE-internal-24, UCLA, 1992.
- [3] A. H. Lumpkin, A. S. Johnson, J. Ruan, R. M. Thurman-Keup, C.-Y. Yao, and P. Evtushenko, “Evidence for anomalous optical transition radiation linear polarization effects in beam-profile monitors”, *Phys. Rev. Spec. Top. Accel. Beams*, vol. 16, no. 10, Oct. 2013. doi:10.1103/physrevstab.16.102801
- [4] B. Yang, “A Design Report For the Optical Transition Radiation Imager for the LCLS Undulator”, SLAC, Menlo Park, CA, USA, Rep. SLAC-TN-10-077, <https://www.slac.stanford.edu/pubs/slactns/tn04/slac-tn-10-077.pdf>
- [5] The Lebow Compnay, <https://lebowcompany.com/>
- [6] Geant4 Collaboration, “Geant4—a simulation toolkit,” *Nucl. Instrum. Meth. A*, vol. 506, no. 3, pp. 250–303, 2003. doi:10.1016/S0168-9002(03)01368-8